Check for updates

Soil nitrous oxide and methane fluxes from a land-use change transition of primary forest to oil palm in an Indonesian peatland

Erin Swails · Julia Drewer · Jodie Hartill ·
Louis-Pierre Comeau · Louis V. Verchot ·
Kristell A. Hergoualc'h

Abstract Despite the documented increase in greenhouse gas (GHG) emissions from Southeast Asian peat swamp forest degradation and conversion to oil palm over recent decades, reliable estimates of emissions of nitrous oxide (N_2O) and methane (CH_4) are lacking. We measured soil fluxes of N_2O and CH_4 and their environmental controls along a peatland transition from primary forest (PF) to degraded drained forest (DF) to oil palm plantation (OP) over 18 months in Jambi, Sumatra, Indonesia. Sampling was conducted monthly at all sites and more intensively following two fertilization events in the OP. Mean annual emissions of N_2O (kg N ha^{-1} yr^{-1}) were 1.7 ± 0.2 for the PF, 2.3 ± 0.2 for the DF and for the OP 8.1 ± 0.8 without drainage canals (DC)

and 7.7 ± 0.7 including DC. High N_2O emissions in the OP were driven by peat decomposition, not by N fertilizer addition. Mean CH_4 annual fluxes (kg C ha^{-1} yr^{-1}) were 8.2 ± 1.9 for the PF, 1.9 ± 0.4 for the DF, and 1.6 ± 0.3 for the OP with DC and 1.1 ± 0.2 without. Considering their 20-year global warming potentials (GWP), the combined non-CO_2 GHG emission (Mg CO_2-equivalent ha^{-1} yr^{-1}) was 3.3 ± 0.6 for the PF and 1.6 ± 0.2 for the DF. The emission in the OP (3.8 ± 0.3 with or without DC) was similar to the PF because reductions in CH_4 emissions offset N_2O increases. However, considering 100-year GWP, the combined non-CO_2 GHG emission was larger in the OP (3.4 ± 0.3 with DC and 3.5 ± 0.3 without) compared to both the PF and the DF (1.5 ± 0.2 and 1.2 ± 0.1, respectively). The increase in peat N_2O emissions associated with the land-use change transition from primary forest to oil palm plantation at our sites provides further evidence of the urgent need to

Responsible Editor: Klaus Butterbach-Bahl.

E. Swails (✉) · K. A. Hergoualc'h
Center for International Forestry Research, Bogor, Indonesia
e-mail: E.SWAILS@CIFOR-ICRAF.ORG

J. Drewer
UK Centre for Ecology & Hydrology, Bush Estate, Penicuik, UK

J. Hartill
School of Biological Science, University of Aberdeen, Aberdeen, UK

L.-P. Comeau
Fredericton Research and Development Centre, Agriculture and Agri-Food Canada, Fredericton, NB, Canada

L. V. Verchot
International Center for Tropical Agriculture, Cali, Colombia

K. A. Hergoualc'h
Centre de Coopération International en Recherche Agronomique Pour le Développement (CIRAD), UMR Eco&Sols, Montpellier, France

protect tropical peat swamp forests from drainage and conversion.

Keywords Tropical · Greenhouse gases · Soil · Drainage · Southeast Asia · Fertilizer

Introduction

Tropical peatlands are crucial for mitigating climate change (Murdiyarso et al. 2013) as they contain a globally important carbon (C) stock of 152–350 Gt C (Gumbricht et al. 2017; Ribeiro et al. 2021) and their disturbance results in vast greenhouse gas (GHG) emissions to the atmosphere (Limpens et al. 2008). Peatlands in the tropics have been widely degraded, with an estimate of 24.7 Mha of natural peatland having been lost between 1850 and 2015, potentially increasing to 36.3 Mha by 2100 (Leifeld et al. 2019). In Peninsular Malaysia, Sumatra and Borneo, where peatlands have been subjected to substantial deforestation and drainage for agriculture including monoculture pulpwood and oil palm plantations only 29% of peatlands (or 4.6 Mha) remained covered by forests in 2015 (Miettinen et al. 2016). Peatlands in Indonesia cover an estimated 13.4–22.5 Mha (Anda et al. 2021; Gumbricht et al. 2017) and have faced extensive threat from reclamation for decades. According to Miettinen et al. (2016), only 7% of pristine peat swamp forest remained in Sumatra and Kalimantan in 2015, with degraded areas including drained and logged forest (23%) and areas managed by either industry (24%) or smallholders (25%). In Jambi province of Sumatra, the majority (65%) of areas industrially operated were oil palm plantations.

Lowland peat swamp forests of Eastern Sumatra are typically flooded for the majority of the year and can have a widely fluctuating water table. Nonetheless, they remain dominated by anoxic conditions, resulting in low rates of organic matter decomposition. They are ombrotrophic, with limited nutrients only delivered via precipitation. As a first step of the degradation process, peat forests are selectively logged for valuable timber by either smallholders or industrial groups. Whenever these forests are converted for cultivation, their remaining biomass is burned and drainage canals are constructed to lower and control the water table. Before planting, machinery is commonly used in industrial plantations to compact the peat for a better anchoring of trees or crops. Oil palms are typically planted following a triangular design and fertilized for optimal productivity. In Indonesia, nitrogen (N) fertilizer is generally delivered in form of urea and plantation blocks are usually managed individually for best efficiency given that the oil palm demands change as they age (Comte et al. 2013). Recommended N fertilizer doses for oil palm plantations on peat range from 50 to 100 kg N ha^{-1} yr^{-1} for immature palms ($<$ 3 years) and 120–160 kg N ha^{-1} yr^{-1} after palms reach maturity (Mutert et al. 1999). Fertilizer is typically applied to a limited area around palms where roots are most active, so the actual N application rates in the fertilized zone around palms are much higher on a per area basis.

Studies conducting concurrent measurements of soil fluxes of carbon dioxide (CO_2), nitrous oxide (N_2O) and methane (CH_4) indicated that pristine, degraded and converted peat soils are expected to contribute varying magnitudes of GHG emissions (Inubushi et al. 2003; Hergoualc'h et al. 2020, 2023; Swails et al. 2021). Cultivated peatlands in the tropics have been identified as global hotspots for N_2O, but the magnitude of these emissions is still poorly quantified (Oktarita et al. 2017; Pärn et al. 2018). The main processes leading to soil N_2O emissions are nitrification and denitrification (Davidson et al. 2000). Soil-atmosphere exchanges of N_2O are driven by a number of factors including soil water content, temperature, and labile carbon and N availability (Firestone and Davidson 1989; Skiba and Smith 2000), with useful indicators being soil net N mineralization and nitrification rates (Verchot et al. 2006). Inputs of N via litterfall (Aryal et al. 2015), root turnover (Silver et al. 2005; Varner et al. 2003), or addition of fertilizer (Shcherbak et al. 2014; Oktarita et al. 2017) are likely to stimulate soil N_2O emissions. When N application exceeds crop needs, an exponential rather than a linear response of soil N_2O emissions to increasing N rates can be expected (Shcherbak et al. 2014; Oktarita et al. 2017). Soil moisture and, more specifically, the water-filled pore space (WFPS) is a key indicator of oxygen availability in soils and has an important effect on N_2O emissions (Butterbach-Bahl et al. 2013). Under tropical climates, the optimum WFPS for soil N_2O emissions was estimated to be around 60% but emissions can remain high at values of 80% (van Lent et al. 2019). Denitrification is known to be

more temperature sensitive than N mineralization and nitrification (Butterbach-Bahl et al. 2013). However, in the tropics where the daily and seasonal amplitude of temperature are relatively small, the change in magnitude of N_2O emissions associated with diel temperature changes may be low. Denitrification and nitrification are also influenced by soil pH (Bremnar and Shaw 1958; Verstraete and Focht 1977; Haynes 1986) and salinity (Inubushi et al. 1999).

Methane is emitted or taken up by the soil depending on the balance between methanogenesis and methanotrophy. Methanogenesis is the anaerobic microbial decomposition of organic material which occurs in waterlogged soils or in anaerobic microaggregates, and methanotrophy takes place in parts of the soil where oxygen is available. While the two processes take place simultaneously in soils, methanogenesis is likely to be the dominant process in waterlogged conditions, whereas at WFPS less than 100%, CH_4 is solely produced in anoxic microsites and part of this CH_4 is subsequently oxidized. Methanogenesis is dependent on a number of factors including the quality and supply of the substrate, anaerobic conditions, temperature and availability of alternative terminal electron acceptors (e.g., NO_3^-, SO_4^{-2}), (Bodelier et al. 2000; Couwenberg et al. 2010; Hergoualc'h and Verchot 2014; Melling et al. 2006). Lowering the water table has been reported to substantially reduce net CH_4 fluxes (Hergoualc'h and Verchot 2012, 2014; Hoyos-Santillan et al. 2016; Swails et al. 2021).

N_2O and CH_4 have high global warming potentials (268 and 86 higher than CO_2 on a 20-year time horizon, respectively (Myhre et al. 2013)). Furthermore, the area of drained peatlands in Southeast Asia is large, with increasing development of oil palm plantations on peat. Therefore, it is crucial to put more effort into comprehensively quantifying non-CO_2 GHG emissions in degraded, drained, and converted peat swamp forests, especially in evaluating spatiotemporal variability of fluxes and investigating the mechanisms that regulate this variability. Suitable experimental designs considering factors influencing temporality (e.g., diel cycles in fluxes, seasonality, plantation age) and spatiality (e.g., microtopography, site management) are needed to upscale emissions estimates over larger time (e.g., years, decades) and spatial (e.g., plantation, regional, national) scales. For example, in oil palm plantations peat GHG fluxes differ considerably between the fertilized zone (FZ)

close to palms and the non-fertilized zone (NFZ) between palms (Oktarita et al. 2017; Swails et al. 2021). Long-term (> 6 months) measurements are sparse (Skiba et al. 2020), and studies of the impact of degradation on peat N_2O and CH_4 fluxes in paired sites are rare, with only two studies in Southeast Asia on paired primary forest—oil palm sites, to our knowledge (Cooper et al. 2020; Swails et al. 2021) and one study in paired primary—drained forest sites (Deshmukh et al. 2021). Increased understanding of the processes driving peat GHG fluxes is also needed to inform management decisions and decrease uncertainty in peat GHG emissions estimates.

In this study we investigated monthly soil fluxes of N_2O and CH_4 and their environmental controls along a peat degradation gradient from primary forest to degraded drained forest to oil palm plantation over 18 months in Jambi, Sumatra, Indonesia, with more frequent measurements following two fertilization events in the plantation. Our experimental design considered micro-scale spatial variation which in the primary forest included hummock and hollow microtopography and in the oil palm plantation fertilized and non-fertilized zones as well as drainage canals. Taking this temporal and spatial heterogeneity into account we calculated surface emissions of N_2O and CH_4 and combined non-CO_2 GHG considering 20- and 100-year GWP. Although a 100-year time horizon [GWP of 265 and 28 for N_2O and CH_4, respectively (Myhre et al. 2013)] is the convention for national GHG inventories, a 20-year time horizon may be more appropriate for evaluating impacts of forest degradation that typically occur over 20–30 years in the tropics, and is aligned with the urgent need to reduce emissions to meet temperature goals under the Paris Agreement (Abernethy and Jackson 2022).

Our specific research questions were: (1) How does forest degradation, drainage and further conversion to oil palm affect fluxes of N_2O and CH_4, and what is the combined net effect of non-CO_2 GHG? (2) What are the magnitudes of N-fertilizer induced changes in N_2O and CH_4 fluxes? (3) Which environmental factors affect these fluxes and to what extent? We hypothesized that (1) Emissions of N_2O increase and CH_4 emissions decrease with forest degradation and conversion to oil palm plantations, (2) N-fertilizer induced N_2O and CH_4 fluxes contribute minimally to total combined non-CO_2 GHG in oil palm, and (3) Variation in N_2O and CH_4 fluxes in the three

land-uses is linked to changes in water table depth, soil moisture, soil temperature, and changes in inorganic N availability.

Materials and methods

Study site

Measurements were carried out at three sites representing a typical peatland land-use change transition in Southeast Asia from primary forest, to degraded forest, to oil palm plantation. All three sites were located on a single peat formation in Jambi province on the east coast of central Sumatra, Indonesia (Fig. 1). The climate in the region is humid tropical. Long-term records from the Jambi airport weather station indicated an average annual rainfall of 2466 mm y^{-1}, with June, July and August being the driest months, and a mean minimum and maximum

monthly temperatures of 22.7 °C and 32.7 °C, respectively (Siderius 2004).

The primary forest site (PF) was an undisturbed mixed peat swamp forest located in the core of Berbak National Park (1° 27′ S, 104° 21′ E), 2 km from the Batang-Hari River (Fig. 1). Hydrology at the site is influenced by diel (tidal) ebb dominated water table fluctuations coupled with flooding from precipitation. Dominant tree families in the PF were *Anacardiaceae*, *Annonaceae*, *Bombacaceae* and *Dipterocarpaceae*. The degraded forest site (DF) was a community forest located close to the oil palm plantation site (OP), approximately 60 km west-southwest from the PF (1° 39′ S, 103° 52′ E) (Fig. 1). The DF had been selectively logged and drained previously, but no logging occurred at the site during the study and the canals were overgrown and partially blocked due to lack of maintenance. The vegetation in the DF was characterized by a single canopy and a dense understory dominated by *Pandanus,* an early-successional species indicative of disturbance (Lampela et al. 2016). Tree
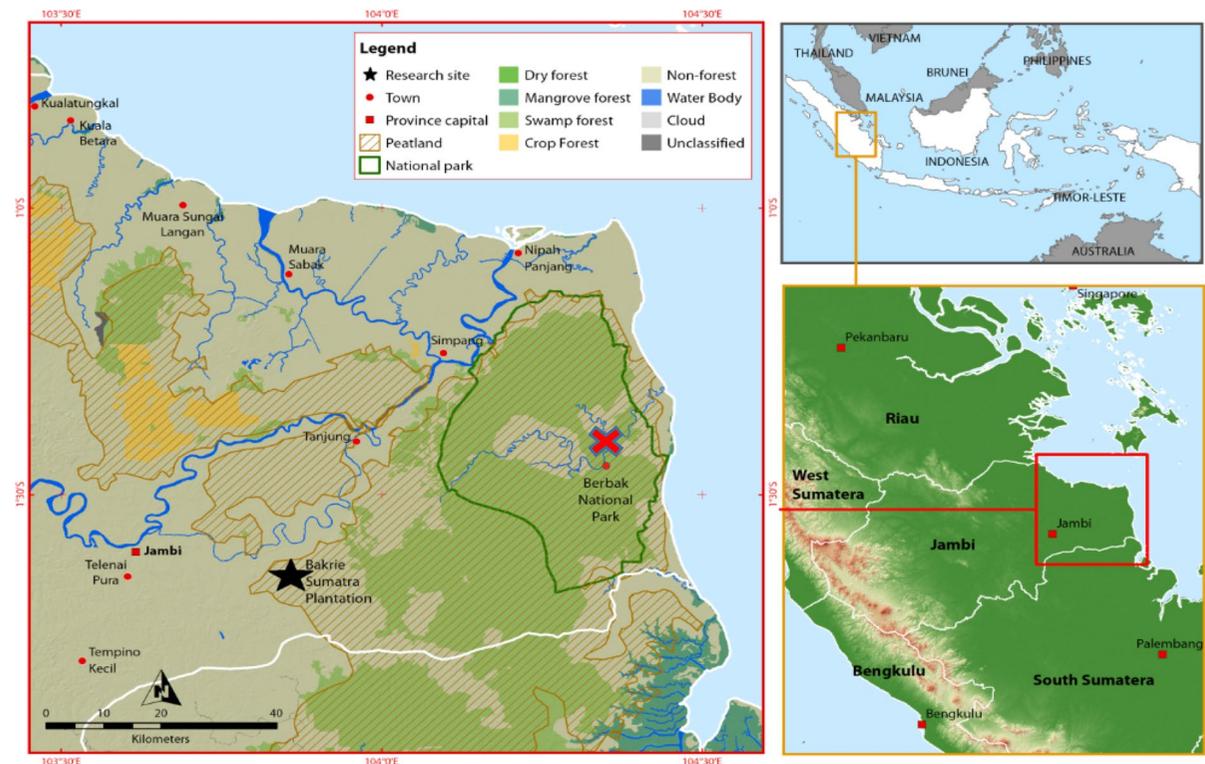
Fig. 1 Location of the study area in Jambi, Sumatra, Indonesia. The black star indicates the location of the degraded forest (DF) and oil palm (OP) sites; the red cross highlights the primary forest (PF) site within Berbak National Park (after Comeau et al. 2021)

species included *Alstonia angustiloba Miq*, *Shorea spp.*, *Koompassia spp.*, and *Tetramerisita glabra Miq*.

The OP was an industrial plantation operated by the company PT Bakrie Sumatera. The site was cleared and burned in 2004 a year before planting in 2005. There were no records of major fire events after initial forest clearance. Palms were planted at a density of 148 palms ha^{-1} in a triangular design with a spacing of 8.8 m between palms. Harvest paths between palm rows alternated with inter-rows where fronds were piled and left to decompose. A main drainage canal of approximately 1.5 m depth was oriented perpendicular to palm rows, with smaller tertiary canals of less than 1 m depth joining the main canal every 8th row. The drainage system was effective at keeping the water table at 50–100 cm below ground surface level. Following the plantation's common practice, palms were fertilized one or two times per year with urea at a rate of 1–1.5 kg palm yr^{-1} equivalent to 68–101 kg N ha^{-1} yr^{-1}. Fertilizer was applied to the area within a 1.5 m radius around the base of the palm, to cover the active roots. Due to supply shortage, palms had not been fertilized for 12 months before measurements began in October 2011. The palms were 7 years old at the beginning of the study.

Sampling regime and soil flux measurements

Our sampling approach was designed to capture within-site temporal and spatial heterogeneity in environmental conditions and soil GHG fluxes. We put emphasis on characterizing monthly variation which is known to be much larger than diel variation (e.g., Günther et al. 2014). Also, three short-term experiments conducted at the sites (detailed information presented in S1) showed no diel variation in soil fluxes of N_2O and CH_4 (Figure S1). We collected measurements once per month from October 2011 until March 2013 in the DF and OP sites with concurrent monthly sampling beginning at the PF site in November 2011. Gas sampling was routinely performed between 10:00 and 13:00. Soil GHG fluxes and environmental variables in the OP site were monitored more intensively following two fertilization events in March 2012 and February 2013. Measurements were collected 1 day before fertilization, the day of fertilization, and 1, 2, 3, 4, 5, 6, 7, 10, 14, 21, 28, and 35 days after both fertilization events, with

additional sampling on days 15, 16, 31 and 32 during the first fertilizer application. Urea was sprinkled onto the bare soil surface in its crystalline form less than 30 min prior to sampling on the day of fertilization. The palms were fertilized at a rate of 0.5 kg urea palm^{-1} (33 kg N ha^{-1}) for the first event and increased to 1 kg palm^{-1} (68 kg N ha^{-1}) for the second event. In total 1.5 kg urea palm^{-1} was applied during the entire 18-month study period (101 kg N ha^{-1}).

Rates of soil CH_4 and N_2O fluxes were determined by the static chamber method (Verchot et al. 1999) using permanently installed opaque white polyvinyl chloride (PVC) chambers (diameter=0.27 m and height<0.3 m). One month before sampling started 10 chamber bases were inserted 5–10 cm into the soil at each site. The chambers in both forests were located within an area covering 50 m^2. The microtopography at the PF site was characterized by alternating raised mounds (hummocks) and depressions (hollows). At this site 6 chambers were installed at randomly determined locations in hollows and 4 were installed on hummocks. In the DF site, the 10 chambers were installed at randomly determined locations across a relatively homogenous microtopography. In the OP site, our sampling design distinguished between the zone within a 1.5 m radius of palms which received fertilizer (FZ) and the NFZ further from palms. At this site, 5 replicate chambers were installed at each position (FZ and NFZ).

The PVC chamber lids included a port for gas sampling and a vent. Samples of air were drawn into 40 ml pre-evacuated glass vials at 0, 10, 20 and 30 min after closing the chamber. The samples were analyzed within 15 days by the Center for International Forestry in Jambi on a Shimadzu 14A gas chromatograph (GC) equipped with an electron capture detector for N_2O and a flame ionisation detector for CH_4 (Loftfield et al. 1997).

In addition, and concomitant with monthly sampling of soil GHG fluxes in the OP site, N_2O and CH_4 fluxes from the main drainage canal were measured at two chambers in the main drainage canal over 1 year, from March 2012 to March 2013, as described in the Supplementary Information (S2).

Peat properties and environmental variables

At each site, shortly before sampling began the peat depth was measured and a pit was dug to 1 m

depth for classification of soil following the international framework by the IUSS Working Group WRB (2006) (Micheli et al. 2006). Three replicate peat samples were collected from the top 20 cm of soil at each pit and analyzed for peat C and N content using a Costech Elemental Combustion System (Costech Analytical 191 Technologies, Inc.) coupled to a Delta V Advantage Mass Spectrometer (Thermo Fisher 192 Scientific Inc.) (Comeau 2016). Samples for determination of peat bulk density using the core method (Grimaldi et al. 2003) were collected from the soil surface (0–6 cm) in November 2011 using a brass sampling ring (inner diameter = 8.15 cm and depth = 6 cm). We collected 5 samples from hollows and 5 from hummocks in the PF site, 10 samples from randomly chosen locations in the DF site, and 5 samples each from FZ and NFZ areas in the OP site. Due to a processing error, hummock samples were lost, therefore we assumed the bulk density of hummocks to be similar to that of hollows as found by Hergoualc'h et al. (2017) in a peat swamp forest of Central Kalimantan.

Hourly rainfall and air temperature were monitored using two weather stations (HD2013, Delta Ohm, Padova, Italy). One was installed at Berbak National Park Simpang Malaka station, approximately 1 km from the PF, and one within the oil palm plantation at the mid-point between the DF and the OP.

Water table depth, air and soil temperature, soil pH, salinity, conductivity, and total dissolved solids, and soil moisture (WFPS) were monitored concurrently with peat GHG flux measurements (monthly and post-fertilization experiments). The water table depth was monitored in a 2 m long PVC pipe (dip well) perforated to allow water flow and installed adjacent (< 75 cm) to each collar. A thermocouple probe (GTH 1170, Greisinger electronic GmBH) was used to measure air temperature, soil temperature to 5 cm depth, and water temperature in the main drainage canal. Peat pH, salinity, conductivity and total dissolved solids were measured to 5 cm depth in the field using a pH electrode with an auto ranging conductivity cell (EC510, Extech©, US). The probe was capable of working on moist peat and, when soils were considered too dry, they were diluted 1:1 with distilled water. Peat samples for moisture content analysis were collected from the top 5 cm adjacent to each collar. Samples were transported to the laboratory, weighed, and oven-dried to constant mass

at 60 °C (Warren et al. 2012; Farmer et al. 2014). After August 2012, a volumetric soil moisture probe (Theta probe, ML2x, Delta T Systems, Cambridge, UK), inserted 5 cm into the peat, was used in the OP in order to prevent excessive disturbance. The probe was calibrated specifically for FZ/NFZ areas with an error margin of ± 0.01%. The probe was not used in the DF and PF where the bulk density was below the probe's optimal working range in organic soils of 0.2–0.7 g cm^{-3}. The WFPS and porosity of samples were calculated using site-specific bulk densities and a default particle density value from the literature of 1.4 g cm^{-3} (Könönen et al. 2015). This resulted in estimated WFPS values over 100% in some instances when measured volumetric soil moisture content was very high.

Litterfall was monitored during 1 year in both forests, from April 2012 to March 2013. Methods for litterfall monitoring in the forests are detailed in the Supplementary Information (S3). Litterfall was not measured in the OP plantation where fronds were cut at harvest time and piled in rows.

Samples for determination of peat inorganic N availability were collected from all sites in March 2013 (day 35 of the second fertilization event in OP plot). One soil sample was collected from the soil surface (0–6 cm) adjacent to each chamber using a brass sampling ring (inner diameter = 8.15 cm and depth = 6 cm). Samples were kept on ice during transportation to the laboratory. We followed the procedure by Hart et al. (1994) to determine net N mineralization and net nitrification rates. For each sample 10 g triplicates were extracted in 100 ml of 2 M KCl to determine inorganic N concentrations. These extracts were shaken for an hour with a rotary shaker and allowed to settle in the dark at room temperature for 24 h. The supernatant was filtered (Whatmann filter paper no. 42) and analyzed for ammonium (NH_4^+) and nitrate (NO_3^-) content at the Indonesian Soil Research Institute in Bogor by spectrophotometry using the indophenol blue method (Solórzano 1969) and the brucine procedure, respectively (EPA 1971). To ascertain net N mineralization and nitrification rates, a further 3×10 g replicates were concurrently taken from the initial sample and incubated in the laboratory in the dark at ambient temperature (28 °C) for 10 days. After 10 days, the incubated sample was extracted according to the procedures described above. The net N mineralization rate was calculated

as the change in inorganic N ($NH_4^+ + NO_3^-$) concentration; the net nitrification rate as the change in NO_3^- concentration. Initial inorganic N stocks were calculated from the first extraction. Soil gravimetric moisture of all samples was measured and the results are reported on a dry mass (d.m.) basis (Oktarita et al. 2017).

Data calculation and presentation

Cumulative rates of peat N_2O and CH_4 fluxes were calculated using linear interpolation between measurement dates (including post-fertilization and diel variation data) and annualized considering 365 days in a year. Annualized fluxes were scaled to the plot-level in the PF and OP considering the proportion of the terrestrial plot area occupied by respectively, hollows/hummocks (50:50) and FZ/NFZ (10:90). Drainage canals were estimated to cover approximately 5% of the area within the NFZ in the OP site, thus a ratio of 10:85:5 coverage of FZ:NFZ:DC was used to estimate emissions including DC fluxes. Errors were computed by Gaussian error propagation (Lo 2005). We considered cumulative rates with non-overlapping standard errors as different.

Cumulative fertilizer-induced N_2O emissions in the OP following fertilization events were calculated using data from the day of fertilizer application until 35 days after fertilization. Cumulative N_2O emissions outside of fertilization periods (non-fertilizer induced) were computed by subtracting the two post-fertilization cumulative emissions from the total cumulative N_2O emissions over the study period.

The annual CH_4 and N_2O fluxes were converted to CO_2-equivalents considering GWPs with climate-carbon feedbacks over time horizons of 20 years (268 and 86 for N_2O and CH_4, respectively) and 100 years (265 and 28 for N_2O and CH_4, respectively) (Myhre et al. 2013).

Statistical analysis

Statistical analysis was performed using R (V4.0.5) software (R Core Team 2017) with a probability threshold of 0.05 to determine significance. Uncertainties are reported as standard errors. N_2O and CH_4 fluxes were calculated from the rate of change in concentration of the analyte in the chamber headspace, determined by linear regression based on the four gas samples (Verchot et al. 1999, 2000). The normality of residuals distribution for peat N_2O and CH_4 fluxes and environmental variables was tested using the Shapiro–Wilk test. Monthly peat GHG fluxes and environmental variables in hummocks, hollows, DF, FZ, and NFZ were compared using the Kruskal–Wallis test. We excluded from the land use comparison, data from the diel and fertilization experiments in the DF and the OP, and measurements of pH, salinity, conductivity, and total dissolved solids at high tide when the PF plot was inundated by the adjacent river. Relationships between monthly GHG fluxes and environmental variables were examined within sites using chamber-scale measurements binned into classes for the independent variables (e.g., 10 cm intervals for the water table depth). Relationships between soil N_2O and CH_4 fluxes and mineral N availability were tested using micro-scale average GHG fluxes in the month of inorganic N measurements.

Results

Peat properties and environmental variables

Peat properties and environmental variables are presented in Table 1. Peat classification reflected more severe soil degradation as land-use intensity increased, with intact wood fragments at the PF site (Lignic) being absent at the drained sites, and loss of the folic (organic) horizon at the OP. Soil bulk density was similar in the forests but significantly higher in the OP ($P < 0.05$, Comeau 2016). Peat C, N, and C:N ratio were homogeneous among the three sites. Peat salinity, conductivity, and total dissolved solids were highest in the PF and lowest in the DF, with intermediate values in the OP, while the opposite was true for pH ($P < 0.001$ for all variables). NH_4^+ dominated soil inorganic N across land-uses and microtopographies and decreased with increasing land-use intensity (PF > DF > OP) ($P < 0.05$). Soil NO_3^- content was similar in both forests, and significantly lower in the FZ of the OP ($P < 0.001$). In the NFZ it was similar to the DF and higher than in the PF ($P < 0.001$). The absolute values of net N mineralization rates tended to be much higher than net nitrification. Net N mineralization increased with increasing land-use intensity (PF < DF < OP) ($P < 0.05$). The net nitrification rate

Table 1 Mean ± standard error (n) of peat properties and environmental parameters for the primary forest (PF), degraded forest (DF) and oil palm plantation (OP) sites

	PF		DF	OP	
	Hummock	Hollow		Fertilized zone	Non-fertilized zone
Peat type[#]	Lignic hemic ombric histosol (Dystric)		Folic hemic histosol (Dystric, drainic)	Hemic histosol (Dystric, drainic)	
Peat depth (m)[#]	4.5		6	6	
Bulk density (g d.m. cm^{-3})	0.16 ± 0.02^a (5)	0.16 ± 0.02^a (5)	0.16 ± 0.01^a (10)	0.21 ± 0.02^b (5)	0.23 ± 0.02^b (5)
C (%)[#]	57.3 ± 3.0 (3)		52.2 ± 1.5 (3)	53.8 ± 0.6 (3)	
N (%)[#]	1.3 ± 0.1 (3)		1.5 ± 0.2 (3)	1.3 ± 0.1 (3)	
C:N[#]	44.0 ± 3.6 (3)		36.3 ± 4.3 (3)	41.9 ± 2.4 (3)	
pH[†]	3.3 ± 0.1^a (33)	3.3 ± 0.0^a (48)	3.7 ± 0.0^c (145)	3.7 ± 0.1^b (73)	3.6 ± 0.0^b (74)
Salinity (ppm)[†]	142.9 ± 8.4^c (29)	145.1 ± 7.0^c (42)	48.4 ± 1.8^a (144)	54.5 ± 1.8^b (74)	53.1 ± 2.7^b (89)
Conductivity (µs)[†]	282.4 ± 16.9^c (29)	277.2 ± 12.4^c (42)	88.4 ± 2.4^a (145)	106.8 ± 3.5^b (74)	102.4 ± 3.6^b (74)
Total dissolved solids (ppm)[†]	197.8 ± 11.3^c (29)	197.4 ± 8.3^c (42)	65.9 ± 3.5^a (145)	75.2 ± 2.3^b (74)	71.6 ± 2.6^b (74)
NH_4^+ content (mg N kg d.m.$^{-1}$)	2999.3 ± 720.9^c (12)	2354.2 ± 220.7^c (18)	1277.5 ± 144.5^b (30)	294.6 ± 66.0^a (15)	199.9 ± 79.0^a (15)
NO_3^- content (mg N kg d.m.$^{-1}$)	21.9 ± 6.0^b (12)	22.3 ± 4.5^b (18)	29.4 ± 6.2^{bc} (30)	6.0 ± 2.2^a (15)	42.7 ± 10.4^c (15)
Net N mineralization rate (mg N kg d.m.$^{-1}$ d^{-1})	-47.6 ± 21.9^a (12)	-37.0 ± 20.1^a (18)	-3.8 ± 16.7^b (30)	14.9 ± 4.3^c (15)	14.2 ± 5.7^c (15)
Net nitrification rate (mg N kg d.m.$^{-1}$ d^{-1})	1.1 ± 1.1^{bc} (12)	3.2 ± 1.1^c (18)	0.2 ± 0.5^b (30)	0.1 ± 0.2^{ab} (15)	-0.1 ± 0.6^a (15)
Water table depth (cm)	27.7 ± 3.1^b (65)	17.9 ± 2.3^a (94)	70.6 ± 1.6^c (169)	79.1 ± 1.2^d (90)	67.2 ± 1.2^c (89)
Peat WFPS (%)	81.7 ± 2.9^c (64)	88.6 ± 1.8^d (93)	44.9 ± 0.8^a (170)	45.6 ± 2.2^a (85)	72.0 ± 2.6^b (83)
Air temp. (°C)	28.3 ± 0.2^a (65)	28.3 ± 0.1^a (94)	29.4 ± 0.2^b (170)	30.9 ± 0.3^c (90)	31.4 ± 0.4^c (89)
Peat temp. (°C)	26.2 ± 0.1^a (65)	26.2 ± 0.1^a (94)	27.0 ± 0.1^b (170)	27.3 ± 0.1^c (90)	27.4 ± 0.1^c (89)
Litterfall (Mg d.m. ha^{-1} yr^{-1})	9.3 ± 0.8 (240)		8.5 ± 1.1 (240)	n/a	
Litterfall (kg N ha^{-1} yr^{-1})	96.0 ± 12.4 (244)		87.6 ± 14.0 (244)	n/a	

Variables are presented per microtopography (hummock/hollow in the PF, Fertilized/Non-Fertilized Zone in the OP). Soil microtopography was homogeneous at the DF site

Letters a–d indicate significant differences between sites and spatial positions. No letters are displayed in the absence of difference

[#]Data from Comeau et al. (2013, 2021) and Comeau (2016)

[†]Excludes for the PF site, high pH (7.6 ± 0.1, n = 60), salinity (167.7 ± 4.7 ppm, n = 60), conductivity (332.6 ± 9.7 ppm, n = 60) and total dissolved solids (233.6 ± 6.9 ppm, n = 60) values from when the site was inundated at high tide of adjacent river. Units of mass are reported as dry matter (d.m.)

was the highest in hollows at the PF, and the lowest in the NFZ area at the OP (P < 0.01).

Over the study period the water table was closer to the peat surface and the soil WFPS was greater in the PF than in the drained sites (P < 0.05 for both variables) (Table 1). Air and soil temperatures were greatest in the OP and lowest in the PF, with intermediate values in the DF (P < 0.05 for both variables). The annual litterfall rate was similar among forest sites and amounted over 18 months (96.0 ± 12.4 and 87.6 ± 14.0 kg N ha^{-1} yr^{-1} in the PF and DF, respectively) to 87–95% of the N-fertilization rate applied

in the OP plantation (101 kg N ha^{-1} yr^{-1}). Monthly dynamic of litterfall is presented in SI3. Monthly variation in rainfall, water table depth, and soil WFPS are reported in SI4. Soil and air temperature monthly variation are detailed in SI5.

Soil nitrous oxide fluxes

Monthly and post-fertilization soil N$_2$O fluxes are displayed in Fig. 2. Average monthly fluxes (g N ha^{-1} d^{-1}) were highest in the NFZ of the OP (24.3 ± 0.4) and lowest in the PF (3.4 ± 0.1 and 5.5 ± 0.1 in hummocks and hollows, respectively) and the FZ of the

OP (4.2 ± 0.1) (P < 0.05). In the DF (6.0 ± 0.1) they tended to be greater but not significantly different from fluxes in PF hollows. In both forests and in the OP FZ and drainage canal (Figure S2) monthly N$_2$O fluxes were < 20 g N ha^{-1} d^{-1} with very few exceptions while the OP NFZ fluxes occasionally exceeded 40 g N ha^{-1} d^{-1} (in Jul, Nov, and Dec 2012). In Nov 2012 there were also noticeable spikes in N$_2$O emissions in the DF and in PF hollows (26.6 ± 9.6 and 24.0 ± 10.0 g N ha^{-1} d^{-1}, respectively)..

Soil N$_2$O emissions in the FZ following the first (F1) and second (F2) fertilization events (average daily flux rates of 10.0 ± 1.0 and 18.4 ± 2.3 g N ha^{-1}
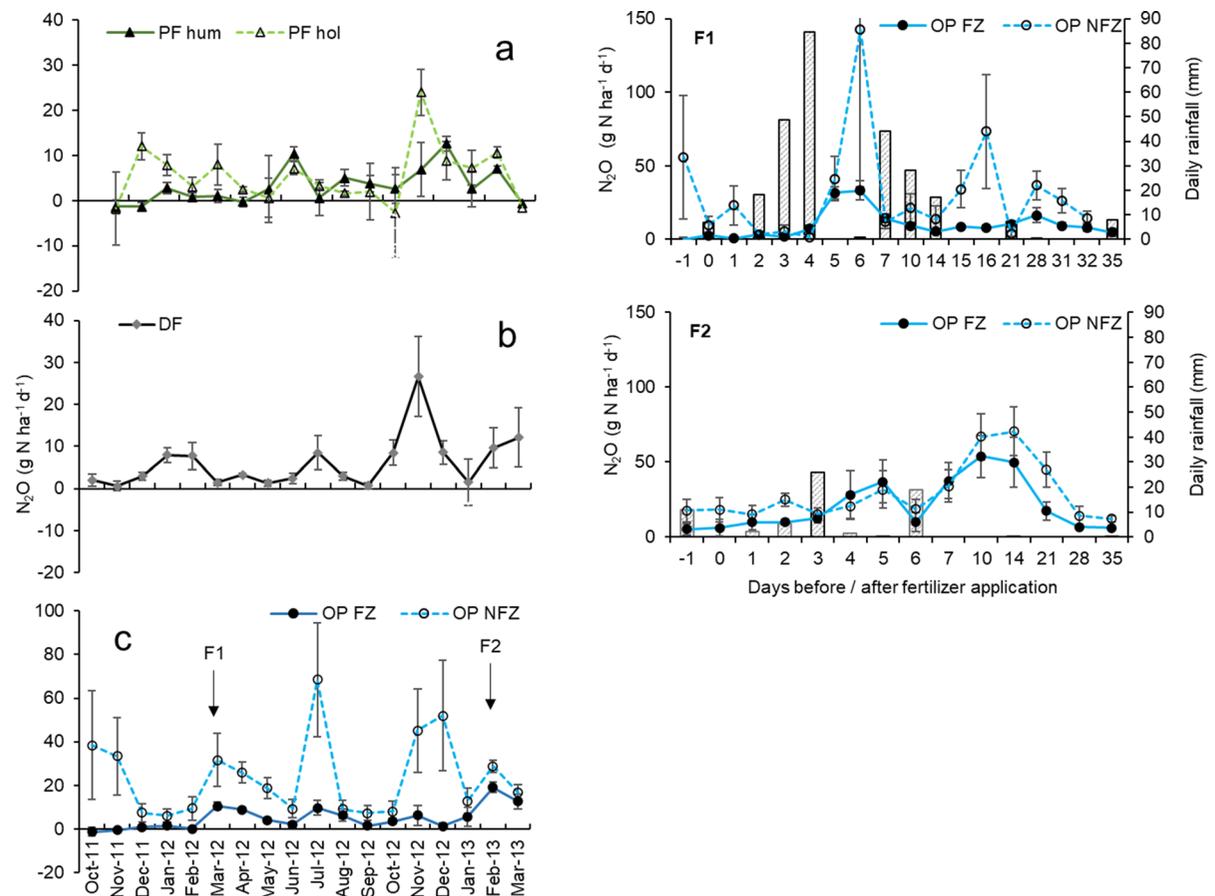
Fig. 2 Monthly mean nitrous oxide (N$_2$O) fluxes in the primary forest (PF) (**a**), degraded forest (DF) (**b**), and oil palm plantation (OP) (**c**) sites. Daily average N$_2$O fluxes and daily rainfall in the OP during two fertilization events (March 2012) (F1) and (February 2013) (F2) are displayed in the insets. Fluxes are presented per microtopography in the PF (hum = hummock, hol = hollow) and in the OP (FZ = Fertilized Zone, NFZ = Non-Fertilized Zone). The soil microtopography in the DF was homogeneous. Error bars represent the standard errors of the means (hum, n = 4; hol, n = 6, DF, n = 10; FZ, n = 5; NFZ, n = 5). The arrows in **c** indicate the two fertilization events in the OP. Please note different scales of y-axes between the forest sites (**a**, **b**) and the OP (**c**)

d^{-1}, respectively) were higher compared to emissions outside of fertilization events (4.1 ± 0.9 g N ha^{-1} d^{-1}) ($P < 0.001$). They were higher after F2 than after F1 when the N application rate was doubled compared to the first event (68 and 33 kg N ha^{-1} applied in F2 and F1, respectively) ($P < 0.001$). In the NFZ fluxes were similar following F2 (27.7 ± 2.7 g N ha^{-1} d^{-1}) and F1 (27.1 ± 5.8 g N ha^{-1} d^{-1}) and after F2 slightly higher than emissions outside of fertilization events (24.6 ± 4.2 g N ha^{-1} d^{-1}) ($P < 0.01$). Peaks in emissions occurred after rainfall events. The emissions in the FZ area peaked in days 5–6 following F1 and two times after F2, at day 5 and 10. Peaks in N$_2$O emissions in the NFZ area occurred three times after F1, at day 6, 16, and 28 and coincided with peaks in the FZ area after F2.

Monthly average N$_2$O flux variation was linked to fluctuations in air temperature in the OP ($P < 0.05$) (Fig. 3a), and to water table depth in forest sites ($P < 0.01$ and $P < 0.001$ in the PF and the DF, respectively) (Fig. 3b). N$_2$O fluxes rose linearly with air temperature in the OP and decreased logarithmically with increasing water table depth in the PF and the DF. Furthermore, micro-scale average N$_2$O fluxes in

March 2013 increased exponentially with increasing net N mineralization across sites ($P < 0.01$) (Fig. 3c).

Site-scale annual soil N$_2$O emissions increased with increasing land-use intensity (PF < DF < OP) (Table 2). They were higher in hollows than hummocks in the PF, and in the OP they were higher in the NFZ than the FZ. Post-fertilization N$_2$O fluxes contributed 69% of cumulative soil emissions in the FZ and 25% in the NFZ, and were equivalent to 26% of site-scale cumulative emissions. Fluxes of N$_2$O from canals generally ranged from small uptakes to emissions of < 5 g N ha^{-1} d^{-1} (Figure S2) and contributed minimally to site-scale N$_2$O emissions in the OP.

Soil methane fluxes

Monthly and post-fertilization CH$_4$ fluxes are displayed in Fig. 4. Average monthly fluxes (g C ha^{-1} d^{-1}) were greatest in the PF hollows (25.3 ± 1.1), followed by hummocks (17.4 ± 0.9) and the OP FZ area (12.0 ± 0.3), and lowest in the DF (5.2 ± 0.1) and OP NFZ area (2.1 ± 0.1) ($P < 0.05$). In the PF, monthly fluxes varied over a wide range in hollows, from large uptakes (-68.6 ± 73.2 g C ha^{-1} d^{-1}, October 2012)
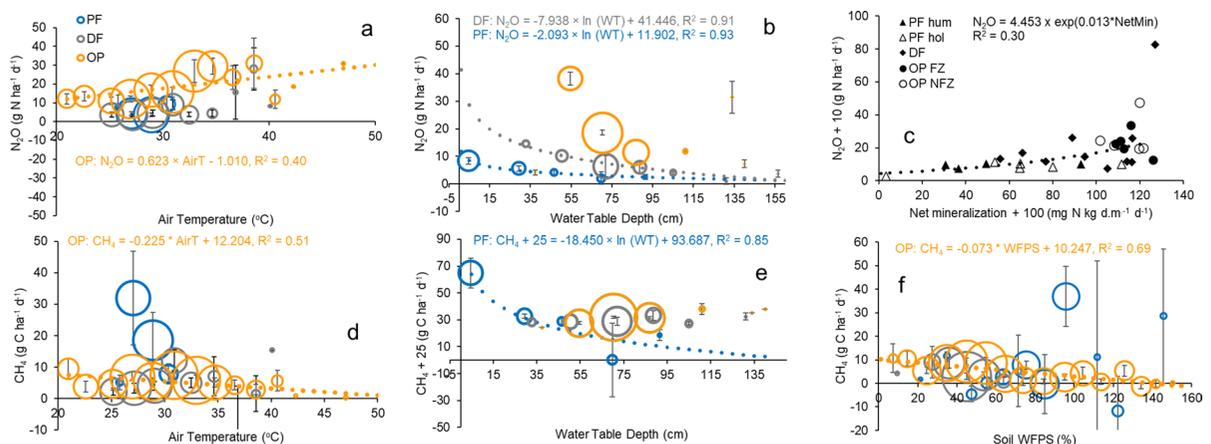
Fig. 3 Relationships between binned monthly non-CO$_2$ greenhouse gas fluxes and environmental variables in the oil palm plantation (OP), drained forest (DF), and primary forest (PF) sites. Relationships between nitrous oxide (N$_2$O) fluxes and air temperature and water table depth are displayed in panels (**a**) and (**b**) respectively. Relationship between daily mean N$_2$O fluxes and net N mineralization (NetMin) in March 2013 across land uses is displayed in **c**. Relationships between methane (CH$_4$) fluxes and air temperature, water table depth, and soil water-filled pore space (WFPS) displayed in panels

(**d**), (**e**), and (**f**), respectively. Very large CH$_4$ fluxes of 139 and 86 kg C ha^{-1} yr^{-1} in the PF at WFPS values > 100% in (f) are not shown. All relationships are significant (p < 0.05). Error bars represent standard error of the mean. The size of the bubbles is relative to the sample size in all panels except (**c**). Fluxes are presented per microtopography in the PF (hum = hummock, hol = hollow) and in the OP (FZ = Fertilized Zone, NFZ = Non-Fertilized Zone) in **c**. The soil microtopography in the DF was homogeneous

Table 2 Annual emissions and standard error (SE) of nitrous oxide (N$_2$O) and methane (CH$_4$) and their 20-year and 100-year global warming potential (GWP) (Mg CO$_2$eq. ha^{-1} y^{-1}) by land-use (LU) in the primary forest (PF), degraded forest (DF), and oil palm plantation (OP) sites calculated by linear interpolation and including microtopographies as spatial effect. Bold text indicates site-scale values

LU	Spatial position	N$_2$O (kg N ha^{-1} y^{-1})	SE	CH$_4$ (kg C ha^{-1} y^{-1})	N$_2$O (20-year GWP)	SE	CH$_4$	SE	N$_2$O+CH$_4$	SE	N$_2$O (100-year GWP)	SE	CH$_4$	SE	N$_2$O+CH$_4$	SE
PF	Hummock	1.2	0.2	7.2	0.5	2.4	2.3	0.8	2.8	0.8	0.5	0.1	0.7	0.2	1.3	0.3
PF	Hollow	2.1	0.3	9.2	0.9	3	2.9	0.9	3.8	1.0	0.9	0.1	0.9	0.3	1.8	0.3
PF	**Site-scale**	**1.7**	**0.2**	**8.2**	**0.7**	**1.9**	**2.6**	**0.6**	**3.3**	**0.6**	**0.7**	**0.1**	**0.8**	**0.2**	**1.5**	**0.2**
DF	**Site-scale**	**2.3**	**0.2**	**1.9**	**1.0**	**0.4**	**0.6**	**0.1**	**1.6**	**0.2**	**1.0**	**0.1**	**0.2**	**0.0**	**1.2**	**0.1**
OP	FZ	1.8	0.1	4.5	0.8	0.7	1.4	0.2	2.2	0.2	0.8	0.1	0.5	0.1	1.2	0.1
OP	NFZ	8.8	0.8	0.7	3.7	0.2	0.2	0.1	3.9	0.4	3.7	0.4	0.1	0.0	3.8	0.4
OP	**Site-scale**	**8.1**	**0.8**	**1.1**	**3.4**	**0.2**	**0.3**	**0.1**	**3.8**	**0.3**	**3.4**	**0.3**	**0.1**	**0.0**	**3.5**	**0.3**
OP	Drainage canal	0.8	0.8	12.3	0.4	5.4	3.9	1.7	4.2	1.7	0.4	0.3	1.3	0.6	1.6	0.6
OP	**Site-scale & DC**	**7.7**	**0.7**	**1.6**	**3.3**	**0.3**	**0.5**	**0.1**	**3.8**	**0.3**	**3.2**	**0.3**	**0.2**	**0.0**	**3.4**	**0.3**

Site emissions (soil flux only) is presented for PF (50:50 hollow:hummock coverage) and OP (10:90 FZ:NFZ coverage). For the OP site, an additional estimate is made including drainage canals (10:85:5 FZ:NFZ:canal coverage)
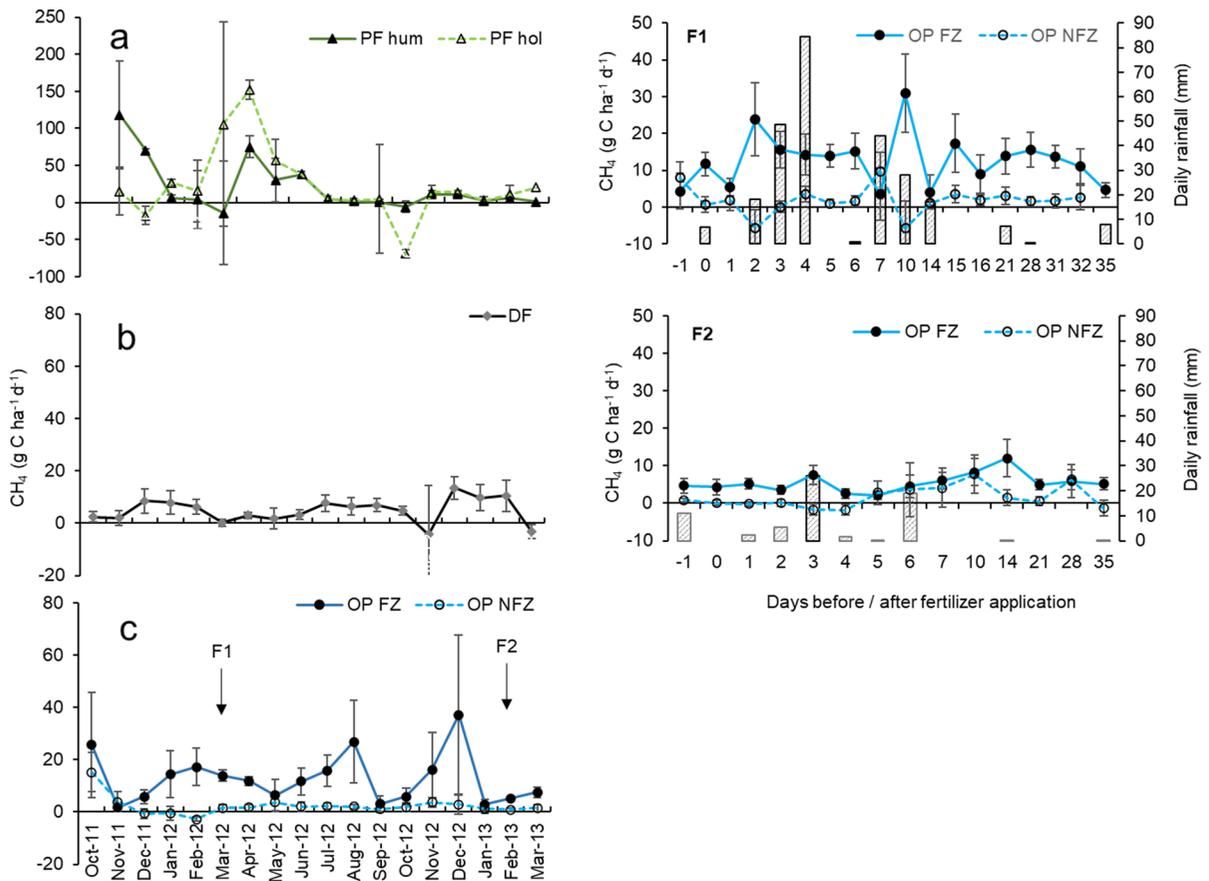
Fig. 4 Monthly mean methane (CH_4) fluxes in the primary forest (PF) (**a**), degraded forest (DF) (**b**), and oil palm plantation (OP) (**c**) sites. Fluxes are presented per microtopography in the PF (hum = hummock, hol = hollow) and in the OP (FZ = Fertilized Zone, NFZ = Non-Fertilized Zone). The soil microtopography in the DF was homogeneous. Error bars represent the standard errors of the monthly means (hum, n = 4; hol, n = 6, DF, n = 10; FZ, n = 5; NFZ, n = 5). The arrows indicate the two fertilization events in the OP. Please note different scales of y-axes between (**a**) and (**b**, **c**)

to large emissions (152.1 ± 138.0 g C ha^{-1} d^{-1}, April 2012). In the drained sites, soil fluxes were rarely greater than 20 g C ha^{-1} d^{-1}. On the other hand, CH_4 fluxes from the canal in the OP exceeded 80 g C ha^{-1} d^{-1} on several occasions (Figure S2). In all three land uses, large pulses of CH_4 emissions from soils were observed in months with high rainfall, and conversely, low CH_4 emissions, or uptake, occurred in months with rainfall < 100 mm.

In the FZ, CH_4 fluxes were lower following F2 (5.3 ± 0.7 g N ha^{-1} d^{-1}) than following F1 and outside of fertilization events (average daily flux rates of 13.1 ± 1.4 g N ha^{-1} d^{-1} and 12.4 ± 2.6 g C ha^{-1} d^{-1}, respectively) (P < 0.001). Fluxes in the NFZ were similar during all periods (2.5 ± 0.7, 1.3 ± 0.9, and 1.1 ± 0.7 g C ha^{-1} d^{-1} for the periods outside

of fertilization events, post F1 and post F2 periods, respectively).

Mean monthly CH_4 fluxes increased as water table rose closer to the soil surface in the PF (P < 0.05) (Fig. 3e). In the OP, CH_4 fluxes increased with decreasing soil WFPS (P < 0.001), but the magnitude of increase was low (8 g C ha^{-1} d^{-1} over the range of measured soil WFPS) (Fig. 3f). CH_4 fluxes in the OP also decreased with increasing air temperature (P < 0.01) (Fig. 3d). Micro-scale variation in average CH_4 fluxes was not related to soil mineral N availability.

Annual site-scale CH_4 fluxes from soils followed an opposite trend to N_2O, with highest emissions fluxes in the PF followed by the DF, and the OP (Table 2). However, considering the contribution of

drainage canal fluxes, site-scale CH_4 fluxes in the OP were not different from the DF. Annual CH_4 fluxes tended to be higher in hollows than hummocks in the PF and were higher in the FZ area compared to the NFZ area in the OP.

Combined changes in nitrous oxide and methane fluxes

Over a 20-year time horizon, site-scale combined non-CO_2 GHG emissions, expressed in units of CO_2 equivalents (CO_2e), were similar in the PF and the OP (regardless of whether drainage canal fluxes were considered), and lower in the DF (Table 2). N_2O made up a relatively larger proportion than CH_4 of site level non-CO_2 GHG emissions in the DF and OP sites (62% and 87%, respectively) but only 21% in the PF site considering 20-year GWP. Considering their 100-year GWP, combined non-CO_2 GHG emissions were similar in the PF and the DF, and higher in the OP, with N_2O dominating non-CO_2 fluxes in the drained sites (83% and 94% in the PF and the DF, respectively). N_2O and CH_4 made more equal contributions in the PF (47% and 53%, respectively) over a 100-year time horizon.

Discussion

Nitrous oxide fluxes and controls

In agreement with a synthesis of prior studies noting the importance of N_2O emissions in tropical wetland forests (van Lent et al. 2015; 2.7 ± 1.9 kg N ha^{-1} yr^{-1}), annual site-scale N_2O emissions in the PF (1.7 ± 0.2 kg N ha^{-1} yr^{-1}) were relatively large. In comparison to regional results, they were higher than values reported in primary peat swamp forests of Sumatra (0.1 ± 0.1 kg N ha^{-1} yr^{-1}, Deshmukh et al. 2021) and Kalimantan (0.9 ± 0.1 kg N ha^{-1} yr^{-1}, Swails et al. 2021). While these forests had annual water table depths comparable to our site, their soil mineral N concentrations ($NH_4^+ + NO_3^-$) were an order of magnitude lower than in this study, potentially explaining the differences in flux magnitude. The control that mineral N substrate availability exerts on N_2O production (Firestone and Davidson 1989; Butterbach-Bahl et al. 2013) was apparent across land-uses with increased N_2O emissions in the

field as rates of net N mineralization rose in laboratory incubations (Fig. 3c). Annual peat emissions of N_2O at the site scale in the DF (2.3 ± 0.2 kg N ha^{-1} yr^{-1}) were substantial, matching other observations in Southeast Asian drained peat swamp forests (4.0 ± 1.6, $n = 6$, Furukawa et al. 2005; Jauhiainen et al. 2012; Takakai et al. 2006; Deshmukh et al. 2021). Site-scale annual soil N_2O emissions in the OP (8.1 ± 0.8 kg N ha^{-1} yr^{-1}) were high, but lower than observations in another block of the same plantation (12.8 ± 2.7 kg N ha^{-1} yr^{-1}, Oktarita et al. 2017) fertilized at a similar rate. Age-related differences in vegetation N-demand (Comte et al. 2013), which increases over the first 10 years after planting (Ng 1977), could explain the lower N_2O emission rate from soils at our site. N uptake by our 7-year-old palms may have been greater compared to the site measured by Oktarita et al. (2017) (3-year-old palms) resulting in less inorganic-N substrate available for N_2O production at our site relative to the younger block.

Observations of N_2O fluxes in tropical peat swamp forests are scarce and rarely disaggregated by microtopography, but the tendency towards higher N_2O emissions from hollows than hummocks in the PF matches findings in undrained Kalimantan forests (Swails et al. 2021). Enhancement of denitrification, the main N_2O production process which is generally favored under anaerobic or reducing conditions (Butterbach-Bahl et al. 2013), may explain the relatively larger N_2O emissions in hollows, where the water table level was closer to the surface than in the hummocks (Table 1). The temporary fertilizer-induced N_2O emissions in the FZ, and the higher emissions from the NFZ throughout the year, suggest that applied N and mineralized N was mostly taken up by the palm in the root zone (FZ) rather than being lost as N_2O. The large contribution of peat decomposition (74%) to total annual site-scale N_2O emissions is consistent with process-based simulations (Swails et al. 2021) and observations (Oktarita et al. 2017; Toma et al. 2011) of cultivated peatlands elsewhere in Indonesia and fertilized similarly to our site.

High concentrations of NH_4^+ and a dominance of NH_4^+ over NO_3^- in the inorganic-N pool (Table 1) is common in wet peat soils (e.g., Hergoualc'h et al., 2020; Oktarita et al. 2017; Swails et al. 2021). This tendency was more pronounced in the undrained PF compared to the drained land-uses (DF and OP), potentially due to oxygen constraints on

transformation of NH_4^+ to NO_3^- by nitrification, an aerobic process. Reduction in soil moisture is also known to stimulate mineralization (Martikainen et al. 1993; Golovchenko et al. 2007; Pärn et al. 2018) which could be induced by peatland drainage, as evidenced by the association between lower soil moisture and higher net N mineralization rates in the drained land-uses (DF and OP) compared to the PF (Table 1).

Increased available substrate for the anaerobic process of denitrification, evidenced by higher peat NO_3^- content in the DF compared to the PF (Table 1), could explain the greater increase in N_2O emissions with rising water table level in the drained than undrained forest (Fig. 3). The lack of response of DF and PF N_2O emissions to air temperature may be related to the narrow range of air temperatures in this land use, as opposed to the OP with different vegetation type where air temperature varied widely.

Increased soil N_2O emissions at drained sites compared to the PF agrees with observations in paired primary forest—drained forest (Deshmukh et al. 2021) and primary forest—oil palm (Swails et al. 2021) peatland sites elsewhere in Southeast Asia. The impact of forest disturbance on microclimate (Blonder et al. 2018; Both et al. 2017; Marsh et al. 2022), which can affect biogeochemical cycling rates (Both et al. 2017), was evidenced by the increase in soil and air temperatures in the DF relative to the PF (Table 1). Conversion to oil palm plantation results in even more drastic changes to vegetation with greatly increased soil and air temperatures compared to forest (Hergoualc'h and Verchot 2014) as observed in our OP site (Table 1). Lowering water table level enhances peat mineralization, which stimulates peat emissions of N_2O as a result of increased availability of mineral N substrate for nitrification and denitrification (Pärn et al. 2018) in addition to the contribution of direct N_2O emissions from N-fertilizers (van Lent et al. 2015). Rising temperature is known to increase rates of nitrification and denitrification (Skiba and Smith 2000), and higher air and soil temperatures in the OP compared to the DF (Table 1) could explain larger N_2O fluxes from peat decomposition in the OP compared to the DF despite similar mean annual water table levels in the two land-uses.

Methane fluxes and controls

Undrained tropical wetlands are widely recognized as important, but uncertain global CH_4 sources (e.g., Ma et al. 2021; Nisbet et al. 2014; Sjögersten et al. 2014; Zhang et al. 2017; 2023). Annual site-scale soil CH_4 fluxes in the PF (8.2 ± 1.9 kg C ha^{-1} yr^{-1}) were substantial and similar to fluxes from other Southeast Asian primary forests (8.7 ± 4.1 kg C ha^{-1} yr^{-1}, Swails et al. 2021). Emissions of CH_4 in the DF (1.9 ± 0.4 kg C ha^{-1} yr^{-1}) were relatively small and comparable to other soil chamber-based measurements in drained peat forests in the region (4.3 ± 2.7 kg C ha^{-1} yr^{-1}, n=4, Furukawa et al. 2005; Hirano et al. 2009; Jauhiainen et al. 2008). There is increasing evidence that vegetation-mediated egress of CH_4 can contribute substantially to ecosystem-scale CH_4 emissions in tropical peat forests (Covey and Megonigal et al. 2019; Pangala et al 2013; Sjogersten et al. 2020). However, the proportion of CH_4 emitted by vegetation may vary by location. For example, emissions of CH_4 measured using eddy-covariance by Sakabe et al. (2018) in an Indonesian peat swamp forest were similar to soil chamber-based CH_4 fluxes measured at the same site by Hirano et al. (2009), indicating a minor contribution of trees to ecosystem-scale CH_4 flux at that site. In the OP the annual CH_4 flux from soil (1.1 ± 0.2 kg C ha^{-1} yr^{-1}) was within the range observed in oil palm plantations on peat in Southeast Asia which varies from net uptake to small emissions (-0.2 to 5.3 kg C ha^{-1} yr^{-1}, n=6, Swails et al. 2021; Lau et al. 2022; Melling et al. 2005).

Higher CH_4 emissions from hollows than hummocks in the PF is consistent with previous observations in the region which linked microspatial variation in CH_4 fluxes from undrained peat forests to soil moisture conditions (Akhtar et al. 2022; Ishikura et al. 2019; Jauhiainen et al. 2008). The activity of methanotrophs is mainly limited by oxygen availability (Le Mer and Roger 2001); therefore higher water table level in hollows (Table 1) can promote methanogenesis over methanotrophy (Inubushi et al. 2003). Contrary to observations in other oil palm plantations on peat (Melling et al. 2006), urea application did not induce transient CH_4 emission increases in the FZ area (Fig. 4). Nonetheless, soil emissions of CH_4 were higher overall in the FZ compared to the NFZ, potentially as the result of labile C inputs by palm roots,

despite drier soils conditions (Table 1) which favors CH_4 consumption over CH_4 production (Le Mer and Roger 2001). Indeed, methanogenesis is often fuelled by recent plant photosynthate (Bridgham et al. 2013). Repeated N addition may have also contributed to higher long-term CH_4 emissions from the root zone either through the stimulation of root growth or alternatively through changes to the microbial community.

Given that methanogenesis and methanotrophy are known to occur simultaneously in soils, the lack of response of CH_4 emission rate to variation in water table depth in the DF and OP, where the water table level was usually well below the soil surface, could be explained by a predominance of methanotrophy in surface peat layers, as opposed to the PF where the water table level frequently approached the soil surface.

In contrast to soil N_2O emissions, which were greater in drained land-uses than undrained forest, drainage and conversion reduced CH_4 emissions in the DF and the OP compared to the PF. Decreased soil CH_4 emissions with lowered water table levels is in agreement with observations from other paired undrained and drained sites in Indonesia (Deshmukh et al. 2021; Swails et al. 2021) and a meta-analysis of soil emission factors for different land-uses on peat in Southeast Asia (Hergoualc'h and Verchot 2014). Even though soil CH_4 fluxes from OP were lower than those from PF and DF, it is noticeable that the net flux was generally positive and not zero or CH_4 uptake as might have been expected from drained sites.

Combined peat non-CO_2 carbon dioxide greenhouse gas emissions

Contrary to a previous meta-analysis of soil GHG emissions from different land-uses in Southeast Asian peatlands, which found reduced non-CO_2 emissions in oil palm plantations compared to undrained forests considering 20-year GWP (Hergoualc'h and Verchot 2014), combined N_2O and CH_4 emissions, expressed as CO_2 equivalents, were similar in our PF and OP over a 20-year time horizon. On the other hand, the 20-year GWP impact of non-CO_2 emissions in the DF was lower than the PF, in agreement with previous findings for the region (Hergoualc'h and Verchot 2014). However, it is important to note that peat swamp forest drainage and conversion to oil palm

plantation is known to result in massive CO_2 emissions from peat decomposition accounting for 90% of the peat GHG budget in drained land-uses of Southeast Asia (Hergoualch and Verchot 2014).

If CH_4 emissions in drained tropical peat forests and oil palm plantations on peat are small to negligible (Drösler et al. 2014), drained nitrogen-rich organic soils in the tropics are known to be a major source of N_2O emission (Pärn et al. 2018). Therefore, N_2O made a much larger contribution than CH_4 to non-CO_2 peat GHG emissions at our drained sites (62% and 87% in the DF and the OP, respectively), and particularly considering the 100-year GWP following norms for GHG inventories (increasing to 83% and 94% in the PF and the DF, respectively). The underlying cause of high N_2O emissions in the OP was not, as often assumed, primarily the added N-fertilizer but peat degradation and decomposition.

In the OP DC N_2O fluxes were minimal and CH_4 emissions (12.3 ± 5.4 kg C ha^{-1} yr^{-1}), were drastically lower than the IPCC default EF (1.6 Mg C ha^{-1} yr^{-1}) (Drösler et al. 2014). Given that the IPCC Tier 1 default for DC emissions is based on a single observation, securing data from additional sites and understanding the underlying mechanisms of emissions from drainage canals would be useful. In our case, DC emissions in the OP increased site-scale CH_4 emissions by 45%, but contributed negligibly to total site-scale non-CO_2 emissions.

Conclusions

This study using an experimental design that considered microscale spatial variability and inter-seasonal variation at all sites, as well as temporary fertilizer-induced increase in OP non-CO_2 emissions, contributes to reducing uncertainty in estimates of the impact of land-use change on tropical peat GHG emissions. However, our study was conducted over a monitoring period of < 2 years in a limited number of sites. Additional studies monitoring soil GHG fluxes and controlling variables over multiple years in sites covering a wide range of environmental conditions are needed to characterize interannual variability in soil fluxes of N_2O and CH_4 and increase understanding of the mechanisms regulating non-CO_2 emissions from pristine, degraded, and

converted tropical peat soils. In particular, studies that disaggregate soil N_2O sources (peat decomposition and emissions induced by N application) in fertilized systems on tropical peatlands are needed. Substantial increases in peat N_2O emissions in the DF and the OP compared to the PF demonstrate the need to include peat emissions of N_2O in inventories of anthropogenic GHG emissions. Although the contribution of non-CO_2 emissions to net peat GHG budgets (10%) in disturbed Southeast Asian peatlands is small in relation to CO_2 (90%), N_2O has a much larger GWP (268 and 265 over 20- and 100-year time horizons, respectively) compared to CO_2 and may be amenable to management. The results of this study suggest air temperature and water table level as potential proxies for assessing spatial and temporal variation in N_2O emissions in drained and converted peatlands. The increase in peat N_2O emissions associated with the land-use change transition from undrained peat swamp forest to oil palm plantation at our sites provides further evidence of the urgent need to protect tropical peat swamp forests from drainage and conversion.

Data availability The datasets generated and analyzed during the current study are available in the Dataverse repository, https://doi.org/10.17528/CIFOR/DATA.00290.

Declarations

References

Abernethy S, Jackson RB (2022) Global temperature goals should determine the time horizons for greenhouse gas emission metrics. Environ Res Lett 17(2):024019

Akhtar H, Lupascu M, Sukri RS (2022) Interactions between microtopography, root exudate analogues and temperature determine CO2 and CH4 production rates in fire-degraded tropical peat. Soil Biol Biochem 169:108646

Anda M, Ritung S, Suryani E, Hikmat M, Yatno E, Mulyani A, Subandiono RE (2021) Revisiting tropical peatlands in Indonesia: semi-detailed mapping, extent and depth distribution assessment. Geoderma 402:115235

Aryal DR, De Jong BH, Ochoa-Gaona S et al (2015) Successional and seasonal variation in litterfall and associated nutrient transfer in semi-evergreen tropical forests of SE Mexico. Nutr Cycl Agroecosyst 103(1):45–60

Blonder B, Both S, Coomes DA et al (2018) Extreme and highly heterogeneous microclimates in selectively logged tropical forests. Front for Glob Change 1:5

Bodelier PLE, Roslev P, Henckel T, Frenzel P (2000) Stimulation by ammonium-based fertilizers of methane oxidation in soil around rice roots. Nature 403:421–424

Both S, Elias DM, Kritzler UH et al (2017) Land use not litter quality is a stronger driver of decomposition in hyperdiverse tropical forest. Ecol Evol 7(22):9307–9318

Bremner JM, Shaw K (1958) Denitrification in soil. II. Factors affecting denitrification. J Agric Sci 51:40–52

Bridgham S, Cadillo-Quiroz H, Keller J, Zhuang Q (2013) Methane emissions from wetlands: biogeochemical, microbial, and modeling perspectives from local to global scales. Glob Change Biol 19:1325–1346

Butterbach-Bahl K, Baggs EM, Dannenmann M et al (2013) Nitrous oxide emissions from soils: how well do we understand the processes and their controls? Philos Trans R Soc B 368:20130122

Comeau L-P (2016) Carbon dioxide fluxes and soil organic matter characteristics on an intact peat swamp forest, a drained and logged forest on peat, and a peatland oil palm plantation in Jambi, Sumatra, Indonesia. PhD Thesis, University of Aberdeen.

Comeau L-P, Hergoualc'h K, Smith JU, Verchot L (2013) Conversion of intact peat swamp forest to oil palm

plantation: effects on soil CO_2 fluxes in Jambi, Sumatra. CIFOR Working Paper 110.

Comeau L-P, Hergoualc'h K, Verchot LV (2021) Dataset on soil carbon dioxide fluxes from an incubation with tropical peat from three different land-uses in Jambi Sumatra Indonesia. Data Brief 39:107597

Comte I, Colin F, Grünberger O et al (2013) Landscape-scale assessment of soil response to long-term organic and mineral fertilizer application in an industrial oil palm plantation, Indonesia. Agr Ecosyst Environ 169:58–68

Cooper HV, Evers S, Aplin P et al (2020) Greenhouse gas emissions resulting from conversion of peat swamp forest to oil palm plantation. Nat Commun 11:407

Couwenberg J, Dommain R, Joosten H (2010) Greenhouse gas fluxes from tropical peatlands in south-east Asia. Glob Change Biol 16:1715–1732

Covey KR, Megonigal JP (2019) Methane production and emissions in trees and forests. New Phytol 222(1):35–51

Davidson EA, Keller M, Erickson HE et al (2000) Testing a conceptual model of soil emissions of nitrous and nitric oxides: using two functions based on soil nitrogen availability and soil water content, the hole-in-the-pipe model characterizes a large fraction of the observed variation of nitric oxide and nitrous oxide emissions from soils. Bioscience 50:667–680

Deshmukh CS, Julius D, Desai AR et al (2021) Conservation slows down emission increase from a tropical peatland in Indonesia. Nat Geosci 14:484–490

Drösler M, Verchot L, Freibauer A et al (2014) Drained inland organic soils (Chapter 2). In: Hiraishi T, Krug T, Tanabe K, Srivastava N, Baasansuren J, Fukuda M, Troxler TG (eds) 2013 supplement to the 2006 IPCC guidelines for national greenhouse gas inventories: wetlands. IPCC, Switzerland

EPA (1971) Methods for the chemical analysis of water and wastes (MCAWW) (EPA/600/4-79/020). EPA Method 375

Farmer J, Matthews R, Smith P et al (2014) Comparison of methods for quantifying soil carbon in tropical peats. Geoderma 214:177–183

Firestone MK, Davidson EA (1989) Microbiological basis of NO and N_2O production and consumption in soil. In: Andreae MO, Schimel DS (eds) Exchange of trace gases between terrestrial ecosystems and the atmosphere. Wiley, New York, pp 7–21

Furukawa Y, Inubushi K, Ali M et al (2005) Effect of changing groundwater levels caused by land-use changes on greenhouse gas fluxes from tropical peat lands. Nutr Cycl Agroecosyst 71:81–91

Golovchenko AV, Tikhonova EY, Zvyagintsev DG (2007) Abundance, biomass, structure, and activity of the microbial complexes of minerotrophic and ombrotrophic peatlands. Microbiology 76:630–637

Grimaldi M, Schroth G, Teixeira WG et al (2003) Soil structure. In: Schroth G, Sinclair FL (eds) Trees, crops and soil fertility concepts and research methods. CABI Publishing, Bristol

Gumbricht T, Roman-Cuesta RM, Verchot L et al (2017) An expert system model for mapping tropical wetlands and peatlands reveals South America as the largest contributor. Glob Change Biol 23:3581–3599

Günther AB, Huth V, Jurasinski G, Glatzel S (2014) Scale-dependent temporal variation in determining the methane balance of a temperate fen. GHG Measure Manage 4:41–48

Hart SC, Stark JM, Davidson EA, Firestone MK (1994) Nitrogen mineralization, immobilization and nitrification. In: Weaver RW, Angle S, Bottomley P, Bezdicek D, Smith S, Tabatabai A et al (eds) Methods of soil analysis: part 2 microbial and biochemical properties. Soil Science Society of America, Madison, pp 985–1018

Haynes RJ (1986) Nitrification. Mineral nitrogen in the plant-soil system. Elsevier, New York, pp 127–165

Hergoualc'h KA, Verchot LV (2012) Changes in soil CH4 fluxes from the conversion of tropical peat swamp forests: a meta-analysis. J Integr Environ Sci 9:31–39

Hergoualc'h K, Verchot LV (2014) Greenhouse gas emission factors for land use and land-use change in Southeast Asian peatlands. Mitig Adapt Strat Glob Change 19:789–807

Hergoualc'h K, Hendry DT, Murdiyarso D, Verchot LV (2017) Total and heterotrophic soil respiration in a swamp forest and oil palm plantations on peat in Central Kalimantan, Indonesia. Biogeochemistry 135:203–220

Hergoualc'h K, Dezzeo N, Verchot LV et al (2020) Spatial and temporal variability of soil N_2O and CH_4 fluxes along a degradation gradient in a palm swamp peat forest in the Peruvian Amazon. Glob Change Biol 26:7198–7216

Hergoualc'h K, van Lent J, Dezzeo N et al (2023) Major carbon losses from degradation of Mauritia flexuosa peat swamp forests in western Amazonia. Biogeochemistry. https://doi.org/10.1007/s10533-023-01057-4

Hirano T, Jauhiainen J, Inoue T, Takahashi H (2009) Controls on the carbon balance of tropical peatlands. Ecosystems 12:873–887

Hoyos-Santillan J, Lomax BH, Large D, Turner BL et al (2016) Quality not quantity: organic matter composition controls of CO_2 and CH_4 fluxes in neotropical peat profiles. Soil Biol Biochem 103:86–96

Inubushi K, Barahona MA, Yamakawa K (1999) Effects of salts and moisture content on N_2O emission and nitrogen dynamics in Yellow soil and Andosol in model experiments. Biol Fertil Soils 29:401–407

Inubushi K, Furukawa Y, Hadi A et al (2003) Seasonal changes of CO_2, CH_4 and N_2O fluxes in relation to land-use change in tropical peatlands located in coastal area of South Kalimantan. Chemosphere 52:603–608

Ishikura K, Hirata R, Hirano T et al (2019) Carbon dioxide and methane emissions from peat soil in an undrained tropical peat swamp forest. Ecosystems 22(8):1852–1868

Jauhiainen J, Limin S, Silvennoinen H, Vasander H (2008) Carbon dioxide and methane fluxes in drained tropical peat before and after hydrological restoration. Ecology 89:3503–3514

Jauhiainen J, Silvennoinen H, Hämäläinen R et al (2012) Nitrous oxide fluxes from tropical peat with different disturbance history and management. Biogeosciences 9:1337–1350

Könönen M, Jauhiainen J, Laiho R et al (2015) Physical and chemical properties of tropical peat under stabilised land uses. Mires Peat 16:1–13

Lampela M, Jauhiainen J, Kämäri I et al (2016) Ground surface microtopography and vegetation patterns in a tropical peat swamp forest. CATENA 139:127–136

Lau SYL, Midot F, Dom SP et al (2022) Application of ammonium sulfate affects greenhouse gases and microbial diversity of an oil palm plantation on tropical peat. Archiv Agron Soil Sci. https://doi.org/10.1080/03650340.2021.2022650

Le Mer J, Roger P (2001) Production, oxidation, emission and consumption of methane by soils: a review. Eur J Soil Biol 37:25–50

Leifeld J, Wüst-Galley C, Page S (2019) Intact and managed peatland soils as a source and sink of GHGs from 1850 to 2100. Nat Clim Chang 9:945–947

Limpens J, Berendse F, Blodau C et al (2008) Peatlands and the carbon cycle: from local processes to global implications—a synthesis. Biogeosciences 5:1475–1491

Lo E (2005) Gaussian error propagation applied to ecological data: post-ice-storm-downed woody biomass. Ecol Monogr 75:451–466

Loftfield N, Flessa H, Augustin J, Beese F (1997) Automated gas chromatographic system for rapid analysis of the atmospheric trace gases methane, carbon dioxide, and nitrous oxide. J Environ Qual 26:560–564

Ma S, Worden JR, Bloom AA et al (2021) Satellite constraints on the latitudinal distribution and temperature sensitivity of wetland methane emissions. AGU Adv 2(3):408

Marsh CD, Hill RA, Nowak MG et al (2022) Measuring and modelling microclimatic air temperature in a historically degraded tropical forest. Int J Biometeorol 66(6):1283–1295

Martikainen PJ, Nykänen H, Crill P, Silvola J (1993) Effect of a lowered water table on nitrous oxide fluxes from northern peatlands. Nature 366:51–53

Melling L, Hatano R, Goh KJ (2005) Methane fluxes from three ecosystems in tropical peatland of Sarawak, Malaysia. Soil Biol Biochem 37:1445–1453

Melling L, Goh KJ, Hatano R (2006) Short-term effect of urea on CH4 flux under the oil palm (*Elaeis guineensis*) on tropical peatland in Sarawak, Malaysia. Soil Sci Plant Nutr 52:788–792

Micheli E, Schad P, Spaargaren O et al (2006) World reference base for soil resources: 2006: a framework for international classification, correlation and communication.

Miettinen J, Shi C, Liew SC (2016) Land cover distribution in the peatlands of Peninsular Malaysia, Sumatra and Borneo in 2015 with changes since 1990. Glob Ecol Conserv 6:67–78

Murdiyarso D, Kauffman JB, Verchot LV (2013) Climate change mitigation strategies should include tropical wetlands. Carbon Manag 4:491–499

Mutert E, Fairhurst TH, Von Uexküll HR (1999) Agronomic management of oil palms on deep peat. Better Crops Int 13:22–27

Myhre G, Shindell, D, Bréon FM et al (2013) Anthropogenic and natural radiative forcing. In: Stocker TF, Qin D, Plattner G-K, Tignor M, Allen SK, Boschung J, Nauels A,

Xia Y, Bex V, Midgley PM (eds) Climate change 2013: the physical science basis. Contribution of working group I to the fifth assessment report of the intergovernmental panel on climate change. Cambridge, Cambridge University Press.

Ng SK (1977) Review of oil palm nutrition and manuring—scope for greater economy in fertiliser usage. Oléagineux 32:197–209

Nisbet EG, Dlugokencky EJ, Bousquet P (2014) Methane on the rise—again. Science 343(6170):493–495

Oktarita S, Hergoualc'h K, Anwar S, Verchot LV (2017) Substantial N₂O emissions from peat decomposition and N fertilization in an oil palm plantation exacerbated by hotspots. Environ Res Lett 12:104007

Pangala SR, Moore S, Hornibrook ER, Gauci V (2013) Trees are major conduits for methane egress from tropical forested wetlands. New Phytol 197(2):524–531

Pärn J, Verhoeven JTA, Butterbach-Bahl K et al (2018) Nitrogen-rich organic soils under warm well-drained conditions are global nitrous oxide emission hotspots. Nat Commun 9:1135

R Core Team (2017) R: a language and environment for statistical computing. In: Team RC (ed) R foundation for statistical computing. Vienna, Austria.

Ribeiro K, Pacheco FS, Ferreira JW et al (2021) Tropical peatlands and their contribution to the global carbon cycle and climate change. Glob Change Biol 27(3):489–505

Sakabe A, Itoh M, Hirano T et al (2018) Ecosystem-scale methane flux in tropical peat swamp forest in Indonesia. Glob Change Biol 24:5123–5136

Shcherbak I, Millar N, Robertson GP (2014) Global metaanalysis of the nonlinear response of soil nitrous oxide emissions to fertilizer nitrogen. Proc Natl Acad Sci 111:9199

Siderius C (2004) A hydrological model of the air Hitam Laut watershed and the impact of various land use scenarios. Wageningen University Report. Wageningen University, Wageningen

Silver WL, Thompson AW, McGroddy ME et al (2005) Fine root dynamics and trace gas fluxes in two lowland tropical forest soils. Glob Change Biol 11(2):290–306

Sjögersten S, Black CR, Evers S et al (2014) Tropical wetlands: a missing link in the global carbon cycle? Global Biogeochem Cycles 28(12):1371–1386

Sjögersten S, Siegenthaler A, Lopez OR et al (2020) Methane emissions from tree stems in neotropical peatlands. New Phytol 225(2):769–781

Skiba U, Smith KA (2000) The control of nitrous oxide emissions from agricultural and natural soils. Chemosphere 2(3–4):379–386

Skiba U, Hergoualc'h K, Drewer J et al (2020) Oil palm plantations are large sources of nitrous oxide, but where are the data to quantify the impact on global warming? Curr Opin Environ Sustain 47:81–88

Solórzano L (1969) Determination of ammonia in natural waters by the phenol hypochlorite method. Limnol Oceanogr 14(5):799–801

Swails E, Hergoualc'h K, Verchot L et al (2021) Spatio-temporal variability of peat CH₄ and N₂O fluxes and their contribution to peat GHG budgets in Indonesian forests and oil palm plantations. Front Environ Sci 9:617828

Takakai F, Morishita T, Hashidoko Y et al (2006) Effects of agricultural land-use change and forest fire on N_2O emission from tropical peatlands, Central Kalimantan, Indonesia. Soil Sci Plant Nutr 52:662–674

Toma Y, Takakai F, Darung U et al (2011) Nitrous oxide emission derived from soil organic matter decomposition from tropical agricultural peat soil in central Kalimantan, Indonesia. Soil Sci Plant Nutr 57:436–451

van Lent J, Hergoualc'h K, Verchot LV (2015) Reviews and syntheses: soil N_2O and NO emissions from land use and land-use change in the tropics and subtropics: a meta-analysis. Biogeosciences 12:7299–7313

van Lent J, Hergoualc'h K, Verchot L et al (2019) Greenhouse gas emissions along a peat swamp forest degradation gradient in the Peruvian Amazon: soil moisture and palm roots effects. Mitig Adapt Strat Glob Change 24:625–643

Varner RK, Keller M, Robertson JR et al (2003) Experimentally induced root mortality increased nitrous oxide emission from tropical forest soils. Geophys Res Lett. https://doi.org/10.1029/2002GL016164

Verchot LV, Davidson EA, Cattânio H et al (1999) Land use change and biogeochemical controls of nitrogen oxide emissions from soils in eastern Amazonia. Global Biogeochem Cycles 13:31–46

Verchot LV, Davidson EA, Cattanio JH, Ackerman IL (2000) Land use change and biogeochemical controls on methane fluxes in soils of eastern Amazon. Ecosystems 3:41–56

Verchot LV, Hutabarat L, Hairiah K, Van Noordwijk M (2006) Nitrogen availability and soil N_2O emissions following conversion of forests to coffee in southern Sumatra. Global Biogeochem Cycles. https://doi.org/10.1029/2005GB002469

Verstraete W, Focht DD (1977) Biochemical ecology of nitrification and denitrification. In: Advances in microbial ecology. Springer, Boston, pp 135–214

Warren MW, Kauffman JB, Murdiyarso D et al (2012) A cost-efficient method to assess carbon stocks in tropical peat soil. Biogeosciences 9:4477–4485

Zhang Z, Zimmermann NE, Stenke A et al (2017) Emerging role of wetland methane emissions in driving 21st century climate change. Proc Natl Acad Sci 114(36):9647–9652

Zhang Z, Poulter B, Feldman AF et al (2023) Recent intensification of wetland methane feedback. Nat Clim Chang 13(5):430–433

Publisher's Note Springer Nature remains neutral with regard to jurisdictional claims in published maps and institutional affiliations.